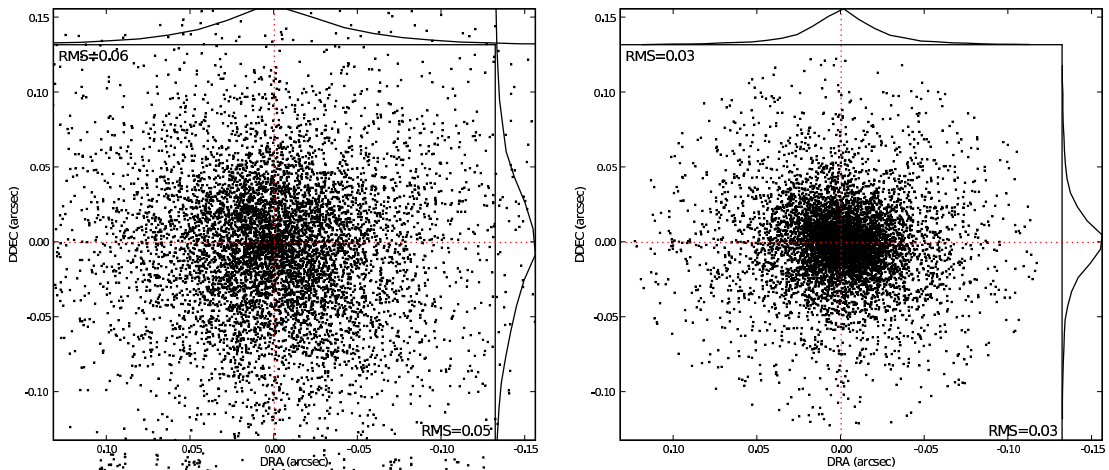# Astro-WISE Astrometry Report

J.P. McFarland, E.R. Deul, E.A. Valentijn, G. Verdoes

Astro-WISE Global Astrometry at Work

Improve[...] astrometric sol[...] [...]point-ings at [...] two-dimensional [...] source position, residuals from astrometrically corrected frames improves from **0.077 arcsec** for the local solutions (left panel) to **0.043 arcsec** for the global solution (right panel).

Document Number: AW-ASTROMETRY-001

Issue Date: March 26, 2008

Abstract

The current status of astrometry in Astro-WISE is explored. This includes the underlying mechanisms, procedures, performance, and accuracies of both the local and the global astrometric solution, as well as the improvement from the local to the global solution. Using all currently Astro-WISE processed data from the WFI instrument on the MPG/ESO 2.2m telescope (24512 frames, more than 3000 exposures), we show that the overall accuracies are consistent with and due to the precision of the USNO-A2.0 reference catalog (**0.3 arcsec** RMS and 1 arcsec systematic) for the local solution and are approximately **0.04 arcsec** for the global solution. In addition, it is found that the precision of the underlying software (SExtractor, LDAC, SWarp) in extracting sources, applying solutions, and regridding frames to 0.200 arcsec per pixel is of the order **0.02 arcsec** RMS. The performance of the local solution has a virtually **100%** success rate with respect to the underlying software, a **98.0%** success rate with respect to the quality of the data, and **96.4%** success rate with respect to the quality of the solution. The predicted precision of any astrometric solution is identical to the actual precision, and this result is repeatable to a level of up to **0.085 arcsec** RMS for the local solution and **0.074** arcsec RMS for the global solution using the extra information in a dither. Finally, the improvement of the astrometric solution from local to global shows an *average* increase in precision of a factor of two, from **0.10 arcsec** to **0.054 arcsec**, in 2-dimensional RMS.

NOTE

The results in this report were created using the new release of astrometry software in Astro-WISE. Both the Python layer and LDAC C-programs have been updated in the current version of the Astro-WISE Environment. Due to improvements in this new release, results relying on astrometry should be reprocessed where necessary, especially those relying on global astrometry. Reprocessing can be done manually through the command-line interface, or in a more automated fashion with the Target Processor (`process.astro-wise.org`).

Contents

1 Introduction

1.1 Overview

This report explores the methods, accuracies, repeatability, and improvement of the astrometric process in the Astro-WISE Information System[1]. It also gives specific use-cases and examples from data processed therein. Section 2 introduces the basics of astrometry in Astro-WISE. Section 3 gives a detailed description of the local solution, the performance of the programs that create the local solution, and the overall results of the local solution in Astro-WISE. Section 4 gives the description, performance, overall results, and improvement of the global solution in Astro-WISE. Section 5 summarizes the most important results found. Lastly, appendix A describes detailed online documentation where further information can be obtained on specific procedures and troubleshooting methods, appendix B describes the astrometric inspection methods used to create many of the figures in this report, and appendix C describes a case study of global astrometry on a set of dithered exposures.

1.2 Considerations

All data used is processed with standard Astro-WISE methods and default settings unless otherwise indicated. Default settings to note are that source extractions are done with a detection threshold of 10 times the background RMS, LDAC.astrom uses a plate polynomial degree (PDEG) of 2 for each local solution and 3 for each global solution, frames that are regridded are done so from the original pixel scale of 0.238 arcsec per pixel to 0.200 arcsec per pixel. It should be noted that comparisons with respect to the pixel size are always done using the original pixel scale unless otherwise stated.

Comparisons with regridded pixel data not only include the pixel scale change, but can show apparently significant qualitative differences in the residual plots using sources extracted from the regridded data despite the use of the same iterative kappa-sigma clipping algorithm. It should be noted that the sources extracted from any two frames using the same settings should be equivalent provided they cover a comparable region of the sky. When compared to different catalogs (e.g., a reference catalog or another extracted catalog), there is no reason to expect a complete point-to-point correspondence, the same number of objects, or the same average values. This is simply because no explicit source matching is done to guarantee a one-to-one correspondence, thus providing a robust, independent comparison of the two sets of data. The result of this is that the figure scaling and the presence of spurious objects between two comparable populations are seldom exactly the same. In most cases, this is obvious and does not affect the comparison.

---

[1] www.astro-wise.org

2 Astrometry in Astro-WISE

Astrometric calibration is a vital, integral part of any astronomical data reduction and analysis system. Astro-WISE performs two kinds of astrometric calibration of pixel data. Their results are termed *local astrometry* and *global astrometry*. The goal of global astrometry is to improve on local astrometry.

The local astrometric solution (see section 3) is derived on the basis of a single chip's information. It is obtained by minimizing the differences between the RA and DEC positions of sources in a single CCD and their positions listed in a catalog of astrometric standards. The global astrometric solution (see section 4) can be obtained if one has dithered observations and local astrometric solutions for each chip. It then additionally minimizes the positional differences of sources appearing on more than one chip. This results in a higher accuracy of the astrometric calibration. The use of Global Astrometry improves the image quality of a coaddition of dithered observations compared to Local Astrometry.

In Astro-WISE, astrometric solutions are solved by running LDAC (Leiden Data Analysis Center) C programs on catalogs extracted from reduced pixel data. The C programs are wrapped in python to allow interaction with the object oriented database model employed by Astro-WISE. In local astrometry, all the steps in the astrometric solution (pre-astrometric correction, association, formal solution, etc.) are handled by the LDAC programs. In global astrometry, all the steps are also handled by LDAC except for the cross-correlation (called association) of sources which is handled by the Astro-WISE database (via advanced queries). This offers a performance advantage because the data to be associated already resides in the database to be used in any combination as needed.

3 Local Astrometry in Astro-WISE

3.1 Description

Local astrometry in Astro-WISE starts with a ReducedScienceFrame that has some basic astrometry, either from the telescope or from the AstrometricCorrection routine upon ingestion. The data from this report is from the Wide-Field Imager (WFI) on the MPG/ESO 2.2m telescope in La Silla Observatory, Chile. Data from this source is subject to large pointing offsets and the AstrometricCorrection procedure was developed directly for the purpose of correcting this data. Data from all other instruments in Astro-WISE can benefit from this tool.

The ReducedScienceFrame is run through the AstrometricParametersTask[2], a Python recipe interacting with the database, whereby various C programs wrapped in Python solve for the astrometry on the catalog level. SExtractor is run to extract the initial catalog. After this, LDAC tools preform all subsequent operations: pre-astrometric fitting to solve for large (approximately arcminute level) offsets, scaling, and rotations using the USNO-A2.0 catalog for reference. This pre-astrometry is then applied to the catalog and it is formally associated with the USNO-A2.0 catalog with offsets that are now on the order of arcseconds. During the process, only the most stellar-like and best quality objects, as determined by SExtractor flags (for saturation, incomplete objects on the edge of a chip, blended objects, etc.) are retained. The catalog is then run through the LDAC.astrom program where the final astrometry is determined[3] and residuals catalog created. The last step is converting the distortion correction to world coordinates prior to storing the solution parameters in the database and the residuals catalog on the dataserver. These final residuals are now on the level of accuracy of the USNO-A2.0[4] catalog: **0.3 arcsec** RMS, **1.0 arcsec** systematic. See section A.1 for a more detailed reference of the steps in this process.

The residuals catalog output from the LDAC.astrom program contains residuals of the form $DRA = RA_{ref} - RA_{ldac}$ and $DDEC = DEC_{ref} - DEC_{ldac}$, where RA_{ldac} and DEC_{ldac} are the coordinates of the extracted sources, corrected for all distortions by the LDAC programs, and RA_{ref} and DEC_{ref} are the coordinates of the reference sources from the USNO-A2.0 catalog. The residual plots created by the AstrometricParameters inspect() method (see figure 1) plot information directly from this residuals catalog and show what is to be the expected precision of the correction when the ReducedScienceFrame is regridded into a RegriddedFrame. This example residuals plot shows a RMS scatter of **0.30 arcsec**, consistent with the USNO-A2.0 catalog's RMS scatter of ≈ 0.3 arcsec.

After the local astrometric solution is created, the information can be applied to create a regridded frame by supplying the ReducedScienceFrame and an external header created from the AstrometricParameters instance to SWarp via a Python wrapper as with SExtractor and LDAC. The outcome of this process, a RegriddedFrame, now has the distortions applied directly to the pixels. In theory, a catalog extracted from such a regridded frame is directly equivalent to the catalog used to create the original solution as output by the LDAC routines (or a catalog extracted from the source ReducedScienceFrame with the AstrometricParameters solution applied at the catalog level). Figure 2 shows an example of the residuals of the source positions between the catalog extracted from a ReducedScienceFrame corrected by the solution via the LDAC routines whose residuals are shown in Figure 1 (RA_{ldac} and DEC_{ldac}) and a catalog extracted from

---

[2]See section A.1 regarding online documentation for AstrometricParametersTask.

[3]As previously indicated, the polynomial degree of the fit, PDEG, is 2 by default for the local solution and 3 for the global solution.

[4]Monet, D. et al., *USNO-A V2.0, A Catalog of Astrometric Standards*, US Naval Observatory Flagstaff Station (USNOFS) and Universities Space Research Association (USRA) stationed at USNOFS, 2000 (http://www.ledas.ac.uk/blasta/usnohelp.php).

a RegriddedFrame that was created using the same astrometric solution (RA_{regr} and DEC_{regr}). As can be seen, the two catalogs agree to within **0.02 arcsec**, or **0.1 pixel**. As a reminder, the pixel scale of the input ReducedScienceFrame and the output RegriddedFrame are 0.238 arcsec per pixel and 0.200 arcsec per pixel, respectively.

This result proves two things: 1) that the derived astrometric solution is applied properly to the ReducedScienceFrame by SExtractor in creating the corrected catalog and to the RegriddedFrame by SWarp, both with a precision of roughly **one tenth of a pixel** in correspondence with the positional extraction accuracy of SExtractor's standard source extraction algorithm, and 2) that the residuals shown in Figure 1 can also apply to the sources from the RegriddedFrame.

To prove this last point more directly, a catalog extracted from the RegriddedFrame and associated with the reference catalog used to derive the original solution, should yield results nearly identical to the astrometric inspection plot shown in Figure 1. Using the residuals notation above, $DRA = RA_{ref} - RA_{regr}$ and $DDEC = DEC_{ref} - DEC_{regr}$, where RA_{regr} and DEC_{regr} are the coordinates of the sources extracted from the RegriddedFrame, and RA_{ref} and DEC_{ref} are the same as above from the reference catalog. Figure 3 shows just such a plot for the RegriddedFrame derived from the solution whose residuals are shown in figure 1. The residuals' RMS values easily match to within **0.02 arcsec**, the approximate RMS from figure 2, with a RMS of **0.30 arcsec** (cf. **0.30 arcsec**).

This proves that the statistics of the individual AstrometricParameters runs derived from the residuals catalog and stored in the database, are a completely valid measure of the statistics of the same solutions if they were applied individually to RegriddedFrames.

Figure 1: Example of an AstrometricParameters inspection plot (see section B.1.1 for details). The plot displays the statistics of the residuals (DRA and DDEC) between the RA and DEC of sources in a source catalog to which the local astrometric solution has been applied and the RA and DEC of those sources as listed in the reference catalog of astrometric standards (USNO-A2.0 in Astro-WISE). The text in the top of the figure lists the observation date (DATE_OBS), the number (N) of sources pairs plotted, their average RA (<RA>) and DEC (<DEC>) in degrees, the average RA and DEC residuals (<DRA> and <DDEC>) and their standard deviations in arcsec, and finally the root-mean-square (RMS) of the two-dimensional residual and the maximum two-dimensional residual (Max) in arcsec. The large upper panel plots DRA versus DDEC. The four panels below it show DRA and DDEC with respect to RA, DEC and pixel coordinates X and Y, respectively. This solution has a RMS value of **0.30 arcsec** for 314 source pairings with the USNO-A2.0 reference catalog, consistent with its RMS of approximately 0.3 arcsec.
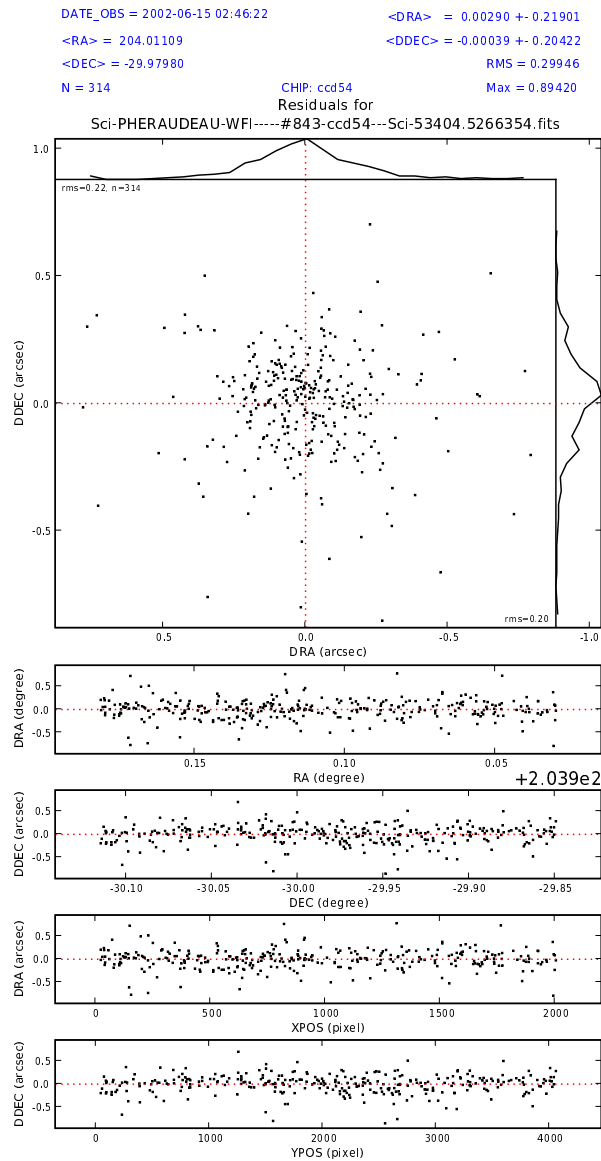
Figure 2: Example of an AstrometricParameters-RegriddedFrame inspection plot (see section B.2.2 for details). The plot displays the statistics of the residuals (DRA and DDEC) between the RA and DEC of sources when the local astrometric solution is applied to a source catalog from a ReducedScienceFrame and the RA and DEC of a source catalog extracted from a Re-griddedFrame to whose pixels this solution has been applied. The text in the top of the figure lists the observation date (DATE_OBS), the number (N) of source pairs plotted, their average RA (<RA>) and DEC (<DEC>) in degrees, the average RA and DEC residuals (<DRA> and <DDEC>) and their standard deviations in arcsec, and finally the root-mean-square (RMS) of the two-dimensional residual and the maximum two-dimensional residual (Max) in arcsec. The large upper panel plots DRA versus DDEC. The four panels below it show DRA and DDEC with respect to RA, DEC and pixel coordinates X and Y, respectively. The plot shows that SExtractor and SWarp applied the astrometric solution correctly to a precision of **0.020 arc-sec** RMS (or approximately 0.1 pixel) for 422 source pairings. (The limits on the panels are purposely matched to those in figure 1 for direct comparison.
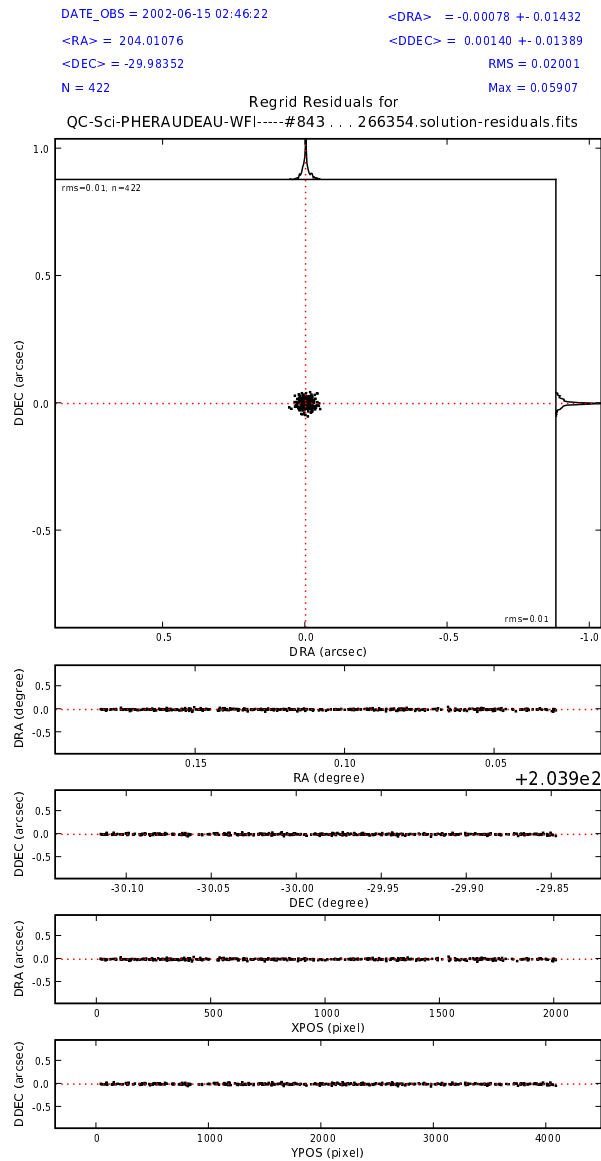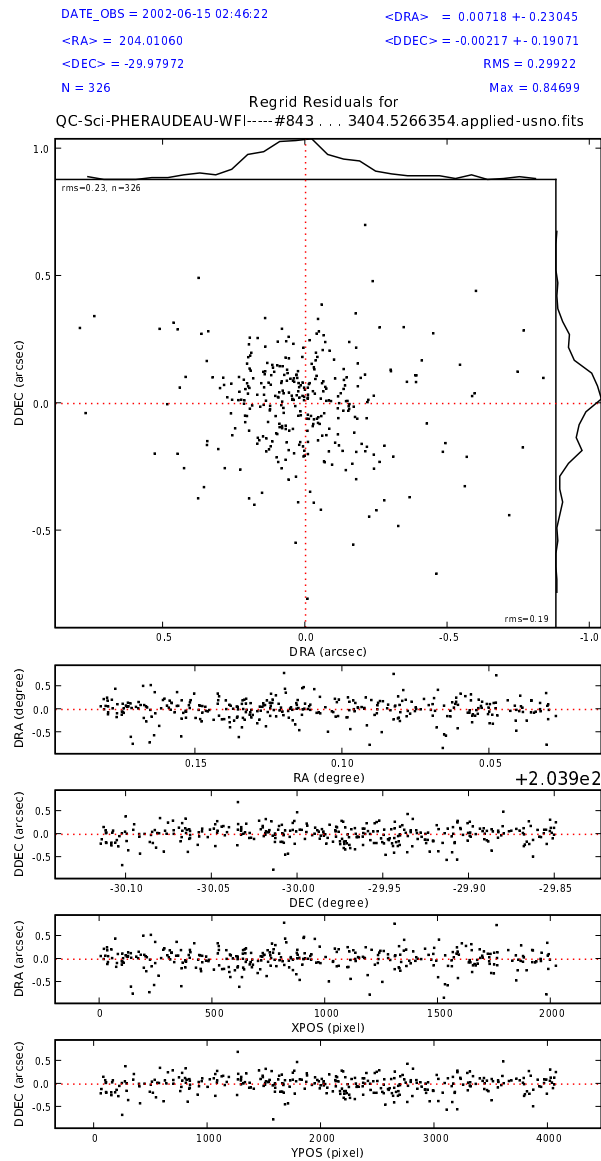
Figure 3: Example of RegriddedFrame residuals inspection plot (see section B.2.1 for details). The plot displays the statistics of the residuals (DRA and DDEC) between the RA and DEC of a source catalog extracted from a RegriddedFrame to whose pixels a local astrometric solution has been applied and the RA and DEC of these sources in the reference catalog of astrometric standards (USNO-A2.0 in Astro-WISE). The text in the top of the figure lists the observation date (DATE_OBS), the number (N) of source pairs plotted, their average RA (<RA>) and DEC (<DEC>) in degrees, the average RA and DEC residuals (<DRA> and <DDEC>) and their standard deviations in arcsec, and finally the root-mean-square (RMS) of the two-dimensional residual and the maximum two-dimensional residual (Max) in arcsec. The large upper panel plots DRA vs DDEC. The four panels below it show DRA and DDEC with respect to RA, DEC and pixel coordinates X and Y, respectively. The residuals show a RMS scatter of **0.30 arcsec** for 326 source pairings with the reference catalog. They **easily agree within 0.02 arcsec** to those in Figure 1. The latter, which are stored in the Astro-WISE database, are thus a good representation of the former.

3.2   Performance

To test the performance of the astrometric solution routine in ASTRO-WISE, the AstrometricParametersTask was run on the most recent version of **24512** ReducedScienceFrames, one for each of RawScienceFrames that have ever been reduced for WFI in ASTRO-WISE as of 19 Feb, 2008. The sample represents fields across the entire visible sky from the MPG/ESO 2.2m telescope in La Silla Observatory, Chile.

Of all the frames processed, only **660 (2.7%)** had problems with LDAC.preastrom. Approximately **two-thirds**, or 425 of those, **had too few sources extracted** from the ReducedScienceFrame which caused the program to exit with an appropriate error, the remaining **one-third** were marked with **poor quality** in the database as explained below. Inspection of a sample of these 660 frames confirmed that problems with **poor initial astrometry** (uncorrected by the AstrometricCorrection routine), **poor guiding resulting in multiple source images**, **shallow exposures resulting in too few extracted sources**, **sparce or inhomogeneous reference source coverage due to extended objects** (large extended galaxies or dense stellar clusters), or **very poor seeing** (> 5 arcsec) caused the failures. The ASTRO-WISE code captures these preastrom errors and sets a quality flag that alerts the calibration scientist to inspect the data (see section B for the available inspection routines). There were a trivial number of failures in LDAC.astrom (only 10) that were caused by marginal data (e.g., poor initial astrometry, guiding problems, or shallow exposures). An additional 643 frames that showed no problems with preastrom were marked with poor quality based on their statistics (see section 3.2.1), and were found to suffer from the same data quality problems mentioned previously. The amount of frames marked with poor quality totaled to **866 (3.6%)** of the frames that were not rejected in the initial step.

3.2.1   Overall Results

The following results are statistics taken from the catalog-level astrometric solution that have been stored in the database and described in section 3.2. The primary diagnostic for the precision of the local solutions are the values of the RMS parameter, the two-dimensional root-mean-square scatter in the DRA, DDEC plane of the reference sources (DRA, DDEC are described in section 3.1). These values are based on the predicted corrections to the pixel data, not the actual corrections. The two should coincide within a reasonable level (0.02 arcsec RMS) as shown near the end of section 3.1. The plots in this section are diagnostic in origin and are used to check the QC limits on local astrometric solutions.

Quality control (QC) limits set for the local solution are that the two-dimensional RMS shall not exceed 1.0 arcsec[5], that the number of extracted-to-reference pairings (NREF) used in the final solution to be in the range $15 < \text{NREF} < 1200$, and that the frame passed the preastrom quality check described in the previous section. Figure 4 shows the RMS of the local astrometric solutions as a function of NREF. It shows a horizontal solid red line at this limit of 1.0 arcsec maximum and a horizontal dashed line at the more desirable limit of 0.3 arcsec. The QC limit on the number of extracted-to-reference source pairings are denoted by the vertical solid blue lines.

This figure has several regions of interest. The solutions at low NREF (below 180) show a high scatter likely due to several factors: too few extracted sources, too few reference sources,

---

[5]req. 551 from *OmegaCAM Data Flow System - Users and programmers manual - PAE 2.11*, found on the ASTRO-WISE website at http://www.astro-wise.org/doc_nova.shtml, states accuracy limited by external reference catalog: USNO-A2.0 has accuracy of ≈ 0.3 arcsec RMS, up to 1 arcsec systematic (see reference in section 3.1).

and small number statistics in the least-squares fit of the astrometric solution. The "tails" beyond NREF of 500 increase in RMS with NREF, mainly due to density problems with both the extracted and reference catalog data. The extracted sources can be of high enough density to allow a dramatic increase in spurious associations due to source crowding. In addition, solutions falling into this higher NREF range can contain large gradients of stellar density (e.g., resolved stellar clusters or unresolved extended sources) accompanied by a lack of sources in these regions in the reference catalog, leading to highly non-uniform spatial coverage. Both spurious associations and deficit of reference sources drive the RMS of the solution up significantly with increasing NREF. The cloud above RMS of 1.5 are from observations of a standard star field using very poor initial astrometry.

Figure 5 zooms in on the region of acceptable QC limits. The region of highest density is below NREF of 160. This region is dominated by solutions with low exposure times and low density of either extracted or reference sources. The exact causes of the scatter in RMS are largely unknown and are under investigation. The region below RMS of 0.5 arcsec shows a more typical distribution with RMS slowly increasing with NREF. These density differences in RMS are better seen in the following histogram plot. The characteristics of the RMS versus NREF plots are not fully understood and require further investigation.

The histogram of the solutions in the region of acceptable QC limits is given in figure 6. The distribution is bimodal with causes not yet fully understood. The larger peak is composed primarily of longer exposure time data ($t > 180$ sec), while the smaller peak is composed primarily of shorter exposure time data ($t \leq 180$ sec). Figure 7 clearly mirrors this dichotomy, showing that the region ± 20 degrees from the celestial equator contains the vast majority of the high RMS solutions (and low exposure time frames). This is the area of ecliptic surveys and photometric standard star fields. Given that the majority of solutions in the smaller peak of figure 6 most likely have been affected by small number statistics and other data-related issues, reducing their RMS by a factor of two would bring them in line with the remainder of the data and show a distribution consistent with mean RMS of 0.3 arcsec, the RMS of the USNO-A2.0 reference catalog.
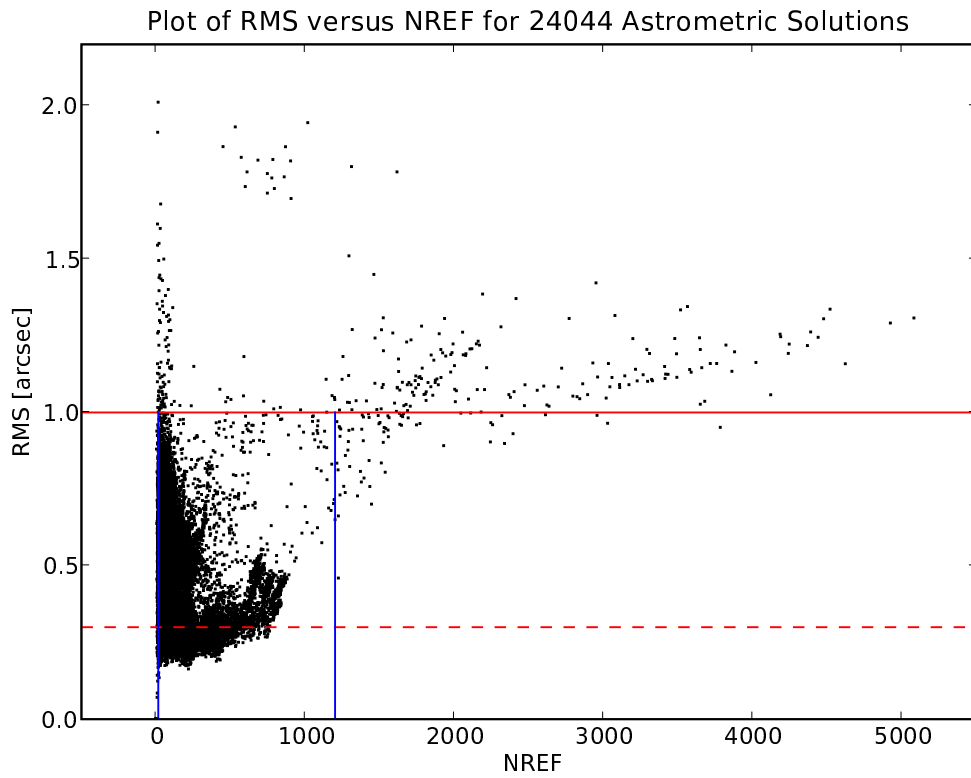
Figure 4: Plot of root-mean-square of residuals (RMS) versus number of identified astrometric standards (NREF) for 24044 local astrometric solutions. The Quality Control accepts solutions which have RMS < 1 arcsec and 15 < NREF < 1200, the region within the solid lines. The horizontal dashed red line at RMS of 0.3 arcsec indicates the RMS of the reference catalog of astrometric standards: USNO-A2.0. The characteristics of the distribution are discussed in detail in section 3.2.1.
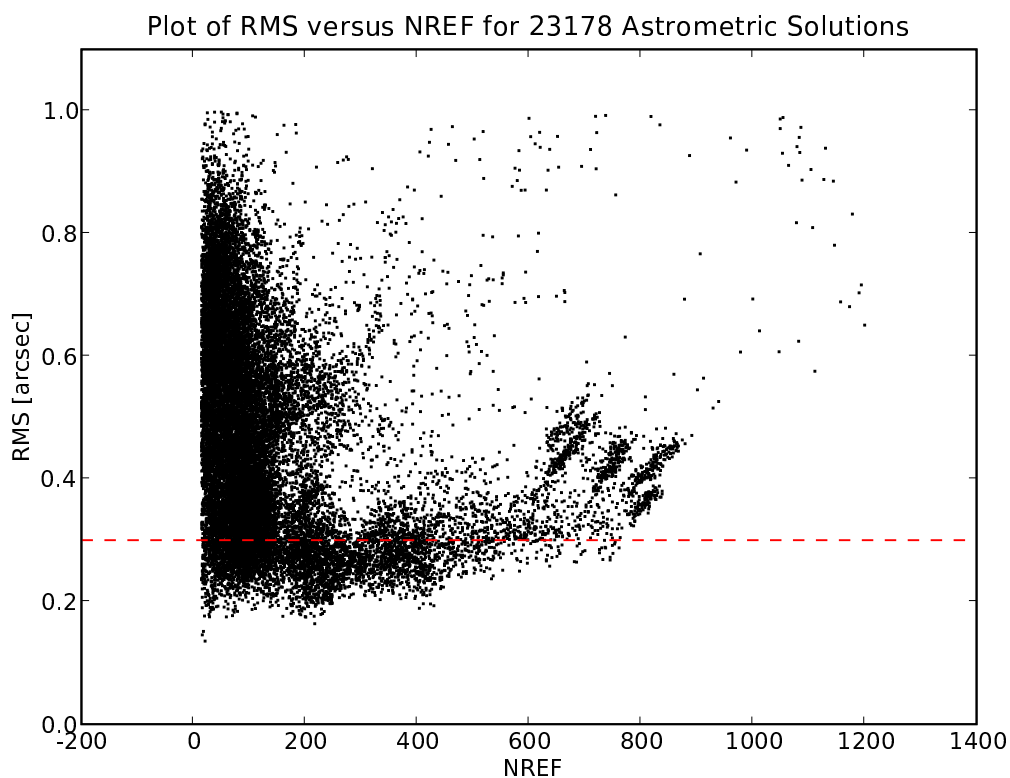
Figure 5: Plot of root-mean-square of residuals (RMS) versus number of identified astrometric standards (NREF) for the 23178 local astrometric solutions which pass the Quality Control. The horizontal dashed red line at RMS of 0.3 arcsec indicates the RMS of the reference catalog of astrometric standards: USNO-A2.0. The characteristics of the distribution are discussed in detail in section 3.2.1.
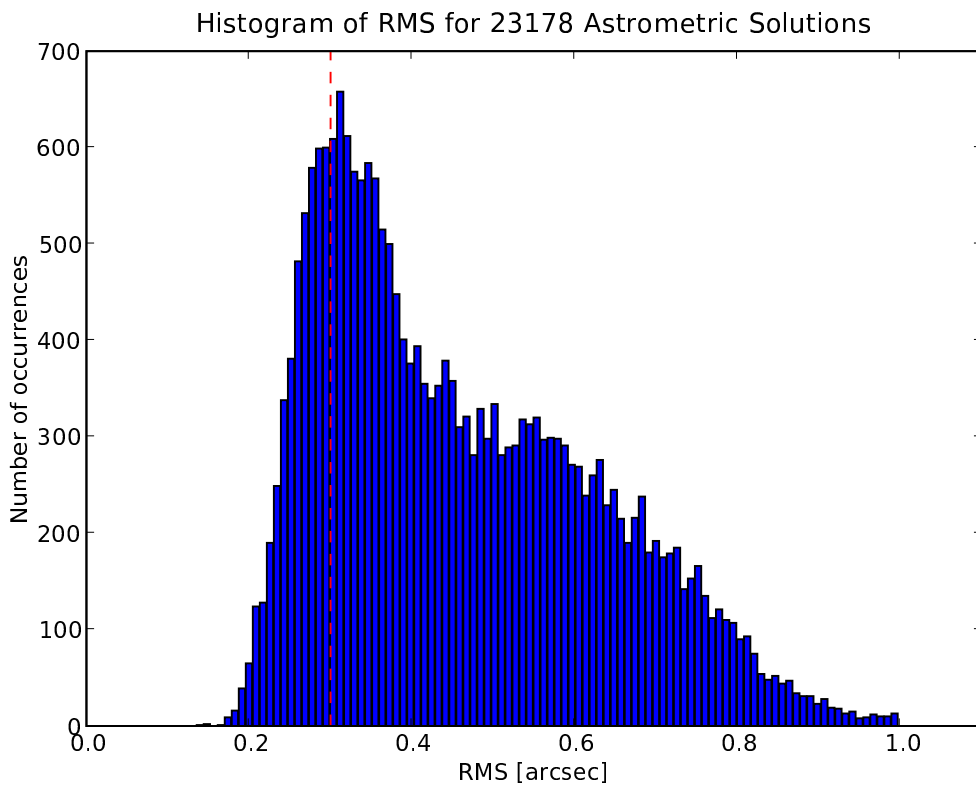
Figure 6: Histogram of RMS for the 23178 local astrometric solutions which pass Quality Control (see figure 5). The vertical dashed red line at RMS of 0.3 arcsec denotes the RMS of the reference catalog of astrometric standards: USNO-A2.0. Approximately 50% of the solutions have a RMS value below 0.4 arcsec. The distribution is bimodal with peaks near 0.3 and 0.6 arcsec. This bimodality is related, in large part, to the exposure times of the source frames (see section 3.2.1).
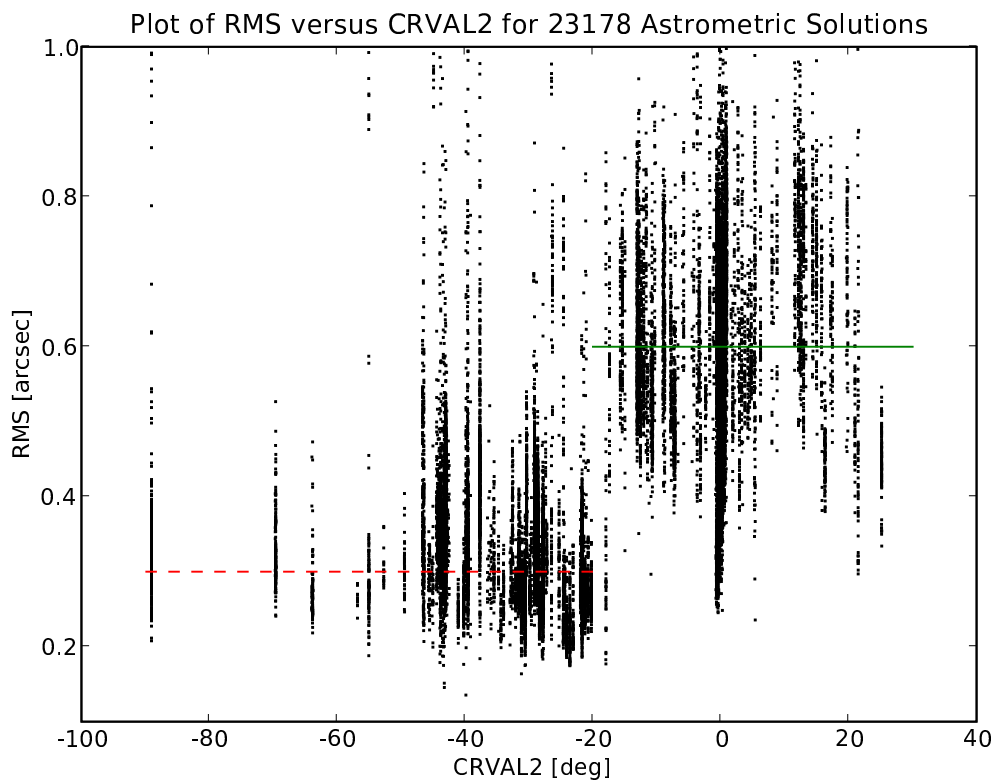
Figure 7: Plot of RMS versus CRVAL2 (declination) for 23178 AstrometricParameters solutions with QC limits applied as in figure 6. The horizontal dashed red line denotes the ideal RMS value of 0.3 arcsec and the horizontal solid green line denotes a value of 0.6 arcsec. It is obvious the vast majority of high RMS solutions occur between a declination of -20 and +20 degrees, the area of ecliptic surveys and common photometric standard fields. See section 3.2.1 for possible causes of the increased RMS in this region.

3.2.2   Repeatability

One method to test repeatability of the local astrometric solution is to compare the sample standard deviation of RMS values for observations of the same field using values stored in the database. This is a catalog-level comparison. A second, more robust method to test repeatability, involves comparing the sources from (Coadded)RegriddedFrames derived from two separate sets of observations of the same field with maximal overlap, where the *local* astrometric solution was used to create the RegriddedFrames. The set of dithered observations used to perform this test here is taken from repeated observations of the field surrounding the Centaurus-A galaxy. Figure 8 shows residuals between the source positions extracted from two CoaddedRegriddedFrames as described in the document *Creating and analysing multi-dimensional data in Astro-WISE environment: a test case* (HTML) found on the Astro-WISE website at http://www.astro-wise.org/doc_nova.shtml. This document plots the declination residual (analogous to DDEC) versus magnitude and shows a 0.05 arcsec RMS scatter after cleaning of the most likely spurious points. Figure 8 adds the DRA component to create the familiar DDEC versus DRA plot. The two-dimensional RMS calculated from the data plotted is **0.085 arcsec**. Because the dithers were virtually on top of each other (a difference of only 50 pixels, or 10 arcsec in world coordinates), this repeatability is the **internal accuracy** of the local solution.

As an additional visualization diagnostic of the repeatability, any two science frames can be compared on the pixel level via image subtraction. Figure 9 shows the difference between two randomly selected, overlapping RegriddedFrames from the Centaurus-A data described above. The figure shows only a small portion of the image (approximately 16 arcmin^2) to highlight any differences between the sources. It should be noted that the sources, despite differences in PSF, overlay each other with an accuracy of less than a pixel. It should also be noted that this varies slightly from region to region and between different frames to a level indicated by the distribution in figure 8.
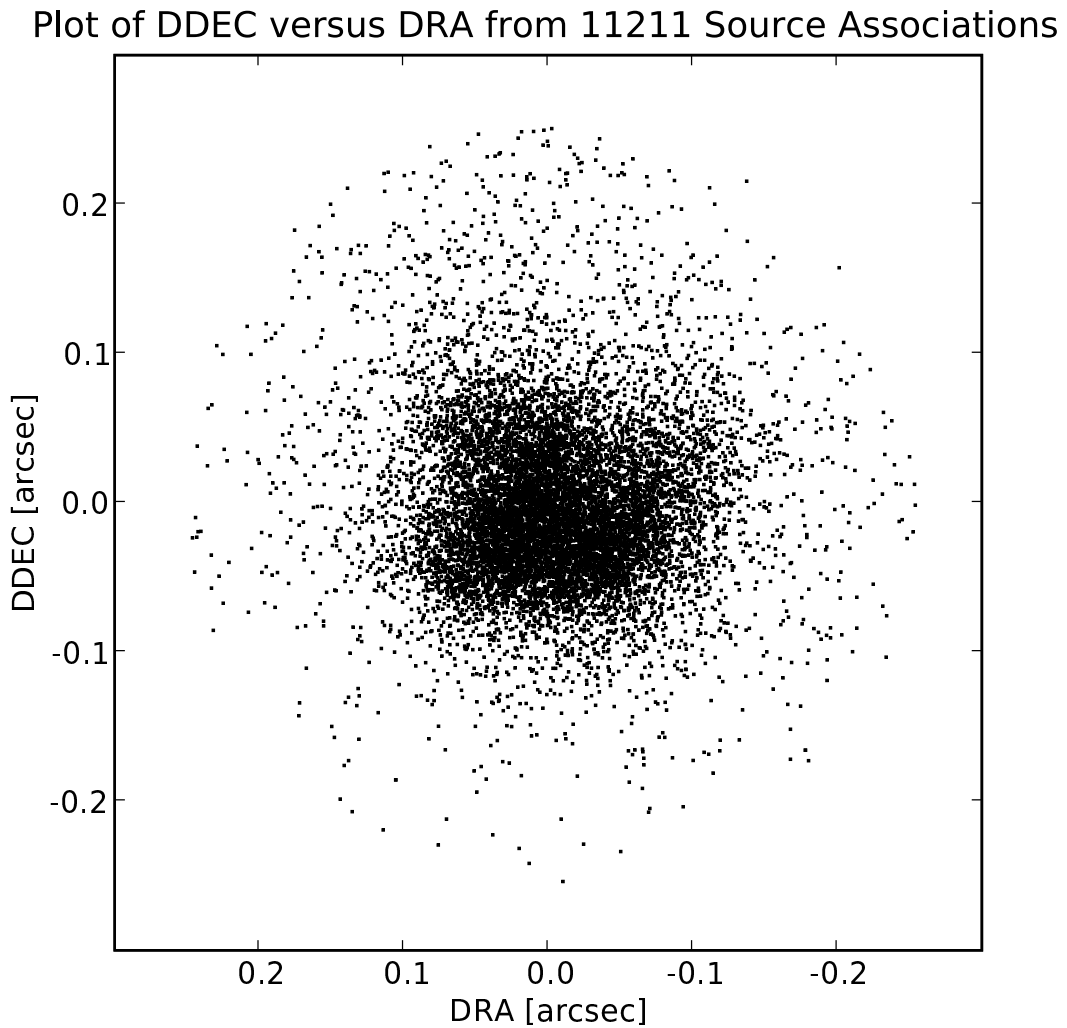
Figure 8: Example of residuals between the source positions of two CoaddedRegriddedFrames, whose source RegriddedFrames were created using *local* astrometric solutions which have the same pointing on two nights. The data plotted has a two-dimensional RMS scatter of **0.085 arcsec** (just over **a third of a pixel**) for 11211 source pairings after iterative clipping at 3 times the RMS (which removes approximately 4% of the pairings). Because the two CoaddedRegriddedFrames have the same pointing, this plot illustrates the internal accuracy of the local solution.

Sci-PHERAUDEAU-WFI-------#844-ccd50-Regr---Sci-53783.6006643.sub0.fits
__MINUS__Sci-PHERAUDEAU-WFI-------#844-ccd50-Regr---Sci-53783.6002816.
sub0.fits
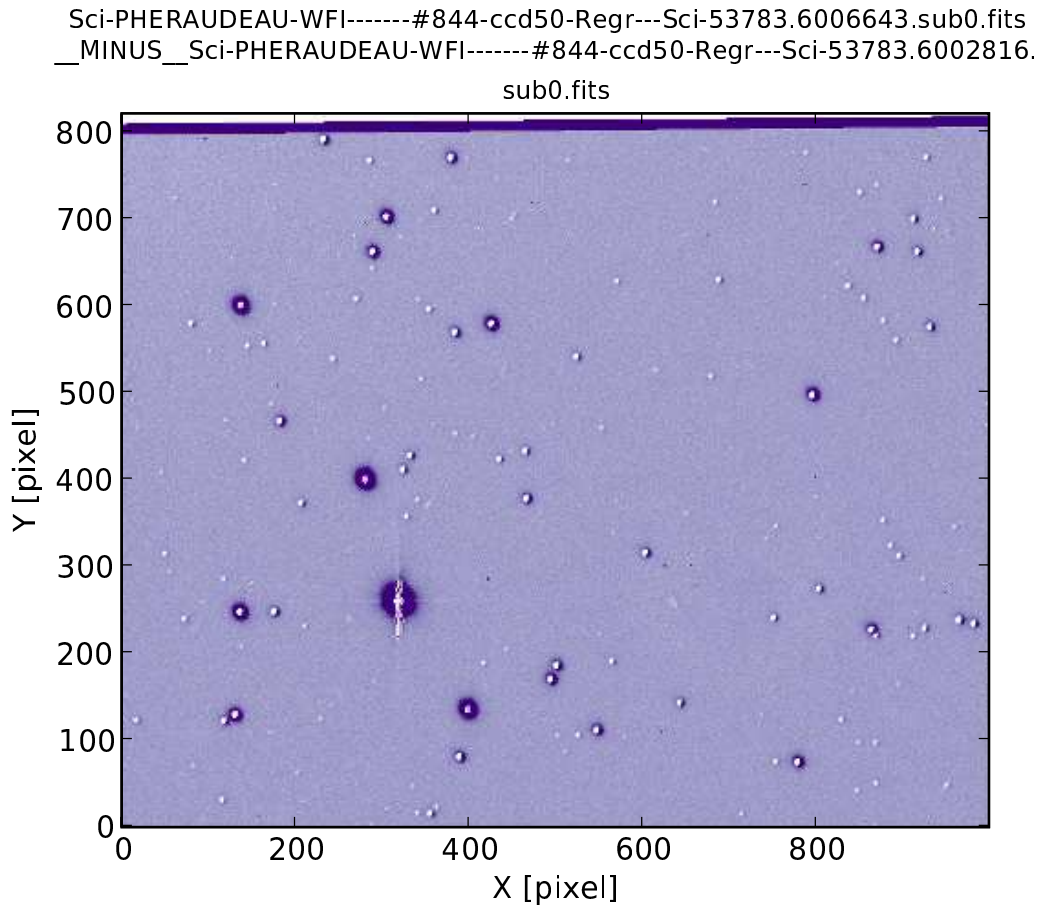
Figure 9: Example of an inspection plot using image subtraction of two RegriddedFrames regridded using the local solution (see section B.3.1 for details). The observations are a subset of those plotted in figure 8. The image excerpt is approximately 4 arcmin on a side (one-eighth of one CCD). As is obvious from the brighter sources, these two frames suffer from a PSF mismatch (no matching was attempted), yet all sources appear to be coincident within less than a pixel (pixel size is 0.200 arcsec).

4 Global Astrometry in Astro-WISE

The most important concept in the global solution in Astro-WISE is that it is *local*. It is local in the sense that it uses the extra information of a set of dithered observations that are closely matched both temporally[6] and spatially (exposures taken within one to two hours with more than 90% of each chip participating in the overlap region, respectively). The extra information characteristic of a closely matched dither consists of the smooth variations in time of the optical system distortions and the large amount of overlap of the detector area. Combining the distortion information with the overlap information allows the global solution to attain the higher precision needed for proper coaddition of the source frames. This *local*-global astrometry is the only method of global astrometry certified in Astro-WISE.

It is very important to understand that the distortions caused by physical changes in the optical system are considered to vary smoothly with time. Any discontinuity in these changes cannot be fit correctly by the polynomial model used in LDAC.astrom. Physical changes within a set of dithered observations are usually continuous, but combining dithers from widely different observation times definitely disrupts the distortion continuity and violates the continuity requirement[7]. Preliminary investigations suggest that one should not expect optimal results (or any results at all!) when combining observations in this way (see the case-study in section C for an example of this).

The process of *global*-global astrometry is quite different. It involves combining those dithers from widely different observation times, using independent derivations of the optical system distortions, but combining all overlap information available from overlapping dithers. It allows for the discontinuity among dithers that the *local*-global process cannot. This type of global astrometry is not supported in Astro-WISE at this time.

4.1 Description

Global astrometry in Astro-WISE starts with the GAstromSourceListTask[8], a DBRecipe that creates GAstromSourceLists from source ReducedScienceFrames using the AstrometricParameters information created by the local solution. This task creates special SourceLists for the specific use by the global astrometric process. Next, the GAstromTask[9] recipe is run. It associates the source position information from the GAstromSourceLists, residing solely in the database, using an AssociateList object. This step replaces the LDAC.associate stage in the local solution. After the association, LDAC.astrom is run on the associated data, and like the local solution, a residuals catalog is created.

The residuals catalog output from the LDAC.astrom program, in this case, contains two sets of residuals, one identical to that of the local solution with respect to the USNO-A2.0 reference catalog (see section 3.1), and the other with respect to the overlapping extracted sources. The latter residuals are of the form $DRA = RA_2 - RA_1$ and $DDEC = DEC_2 - DEC_1$, where RA_1

---

[6]Global astrometry in Astro-WISE is based on the concept of fixed focal-plane geometry. This means that any difference in the focal plane from pointing to pointing is assumed to change in a linear fashion only, with higher order distortions remaining constant (e.g., only relative translations of the entire focal plane in RA and Dec are corrected for). This assumption of fixed focal-plane geometry adds information to the system, benefitting the astrometric solution. Generally, only sets of exposures taken within a short amount of time (generally less than an hour) will match this criteria. This minimizes differences in telescope flexure caused by different altitude and azimuth locations. See the case-study in section C for the implications this concept

[7]See the HOW-TO in section A.5 for the details of how the inter-pointing fitting (Chebychev) polynomial degrees set in the FDEG parameter relate to this issue.

[8]See section A.2 regarding online documentation for GAstromSourceListTask.

[9]See section A.3 regarding online documentation for GAstromTask.

and DEC_1 are the coordinates of the extracted sources from a given frame and RA_2 and DEC_2 are the coordinates of the extracted sources from another pointing, same or different chip, that overlaps the first, both corrected for all distortions by the LDAC.astrom program. The residual plots created by the GAstrometric inspect() method plots both sets of residuals directly from this residuals catalog, both by individual chip and for all chips combined, and shows what is to be the expected precision of the global solution used to combine a set of RegriddedFrames into a CoaddedRegriddedFrame. Figure 10 is a plot of the overlap residuals for all 8 chips of a 4-point dither showing a solution with overlap scatter of **0.04 arcsec** RMS.

After the global astrometric solution is created, the information is used to create a new AstrometricParameters instance for each ReducedScienceFrame that went into the solution. The parameters and statistics for the global solution are computed and stored on a per frame basis and likely will not match those values of other frames from the same solution. As with the local solution, these parameters can be applied to create a regridded frame by supplying the ReducedScienceFrame and an external header created from the AstrometricParameters instance to SWarp via a Python wrapper as with SExtractor and LDAC. The new RegriddedFrame now has the globally-determined distortions applied directly to the pixels. The group of RegriddedFrames created from the new solution parameters can then be coadded into a CoaddedRegriddedFrame with much greater precision than with the local solution only.

In theory, the dispersion of the positional offsets between the RegriddedFrames created using the global solution AstrometricParameters is directly equivalent to the dispersion of the positional offsets between overlapping corrected source catalogs within the global solution (e.g., those shown in the all overlaps residuals plot in Figure 10). Figure 11 shows the residuals of the source positions between catalogs derived from RegriddedFrames created using the global solution Astrometric parameters.

Figure 10 shows the all overlap residuals (predicted precision) for the solution used to create the RegriddedFrames in figure 11 (applied precision). Comparing the two shows that the predicted precision illustrated in the figure 10 is comparable to the actual precision obtained in figure 11 (**0.04 arcsec** RMS in both cases). This is the global version of the test performed at the end of section 3.1 for the local solution residuals.

Figure 10: Example of a GAstrometric (Global Astrometric) solution inspection plot (see section B.1.2 for details) for all eight chips of a 4-point dither. The plot displays the statistics of the residuals (DRA and DDEC) between the corrected RA and DEC of sources extracted from a frame to matching sources extracted from any of the other frames, same or different chip, that overlap the first. The text in the top of the figure lists the observation date (DATE_OBS), the number (N) of sources pairs plotted, their average RA (<RA>) and DEC (<DEC>) in degrees, the average RA and DEC residuals (<DRA> and <DDEC>) and their standard deviations in arcsec, and finally the root-mean-square (RMS) of the two-dimensional residual and the maximum two-dimensional residual (Max) in arcsec. The large upper panel plots DRA versus DDEC. The four panels below it show DRA and DDEC with respect to RA, DEC and pixel coordinates X and Y, respectively. This solution has a RMS value of **0.04 arcsec** (< 0.2 pixel) for 6910 source pairings.

Figure 11: Example of a RegriddedFrame residuals inspection plot (see section B.2.3 for details) for all eight chips of a 4-point dither. The plot displays the statistics of the residuals (DRA and DDEC) between the RA and DEC of sources extracted from a regridded frame to matching sources extracted from any of the other regridded frames, same or different chip, that overlap the first. The text in the top of the figure lists the observation date (DATE_OBS), the number (N) of sources pairs plotted, their average RA (<RA>) and DEC (<DEC>) in degrees, the average RA and DEC residuals (<DRA> and <DDEC>) and their standard deviations in arcsec, and finally the root-mean-square (RMS) of the two-dimensional residual and the maximum two-dimensional residual (Max) in arcsec. The large upper panel plots DRA versus DDEC. The four panels below it show DRA and DDEC with respect to RA, DEC and pixel coordinates X and Y, respectively. This solution has a RMS value of **0.04 arcsec** (< 0.2 pixel) for 7653 source pairings.

4.2   Performance

The nature of the global solution in Astro-WISE allows it to be very robust. Because it is a secondary process to the local solution, only data whose solutions require refining are run through this process, and software failures are exceedingly rare.

4.2.1   Overall Results

In this section, the global solutions of any dither for which a global solution has been calculated for WFI dithered data (22 unique dithers covering 5 fields) and an additional set of global solutions where only the local solution has been calculated (5 dithers of 1 field) are shown. Each point corresponds to one AstrometricParameters object created for each frame by the global solution. All parameters stored therein (e.g., N_OVERLAP, RMS_OVERLAP, etc.) pertain only to that particular frame. The solutions shown here are a summary of all the public global solutions as of 19 Feb, 2008. They have been solved again using the latest version of LDAC and Astro-WISE software with the default settings. The primary diagnostic for the precision of the global solution is the value of the RMS_OVERLAP parameter, the two-dimensional root-mean-square scatter in the DRA, DDEC plane of the overlapping sources (DRA and DDEC for this case are described in section 4.1). These values are based on the predicted corrections to the pixel data, not the actual corrections. The two coincide within a reasonable level of error as shown near the end of section 4.1.

Quality control (QC) limits set for the global solution at this time are that RMS_OVERLAP shall not exceed 0.1 arcsec to be considered an acceptable solution[10] with the additional limits of $20 <$ N_OVERLAP < 20000 to flag solutions with too few associations or excessive source crowding. N_OVERLAP corresponds to the number of associations between the overlapping regions of one source frame with respect to all other overlapping frames that were used in the solution. It is analogous to the NREF parameter in the local solution.

The diagnostic plots in figures 12 & 13 show a dashed line at the desirable limit of 0.05 arcsec. No solutions in this dataset exceeded the **0.1 arcsec** RMS limit. Figure 12 plots RMS_OVERLAP versus N_OVERLAP for AstrometricParameters objects whose parameters were derived from a global solution. All dithered data that was ever used in the creation of a global solution as described above is represented here. Almost **two-thirds of the solutions** are within the ideal quality limit of RMS_OVERLAP of **0.05 arcsec**. Figure 13 is the histogram of the same RMS_OVERLAP data and clearly shows that the data has a nearly normal distribution within the acceptable QC limit region.

---

[10]req. 634 from *OmegaCAM Data Flow System - Users and programmers manual - PAE 2.11*, found on the Astro-WISE website at http://www.astro-wise.org/doc_nova.shtml, states < 0.1 arcsec
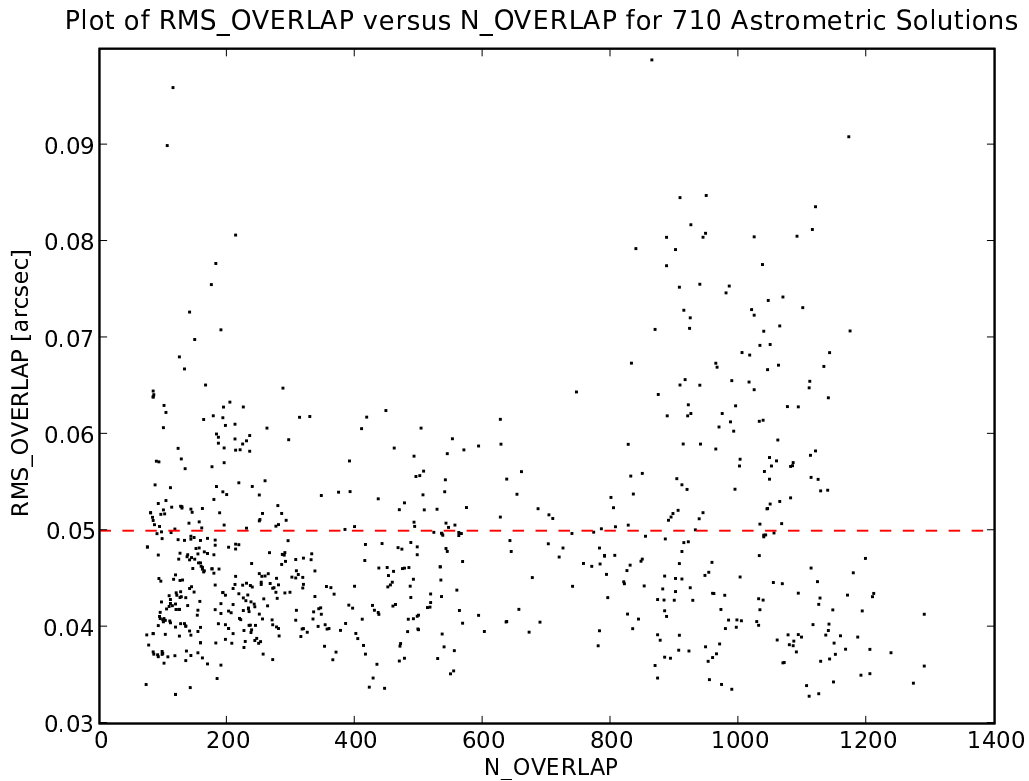
Figure 12: Plot of root-mean-square of residuals (RMS_OVERLAP) versus the number of over-lapping source pairings (N_OVERLAP) for 710 AstrometricParameters objects derived from a global solution. The solutions are from a total of 22 dithers covering 5 fields where global solutions have been previously calculated, and 5 dithers of 1 additional field where only the local solution was previously calculated. These solutions were created using the most recent techniques available. The Quality Control accepts solutions with the same criteria as in the local solution (see 4) which also have RMS_OVERLAP < 0.1 arcsec and 20 < N_OVERLAP < 20000, none of which are exceeded by this dataset. The ideal level of RMS_OVERLAP of **0.05 arcsec** is denoted by the dashed red line. The characteristics of the distribution are discussed in section 4.2.1
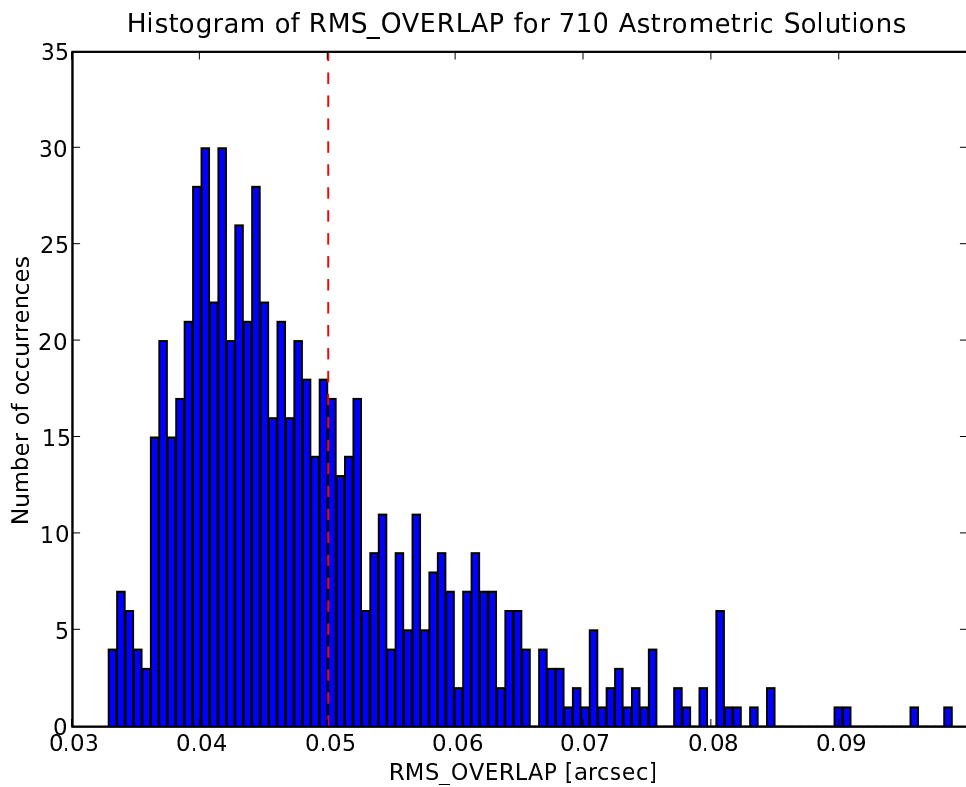
Figure 13: Histogram of RMS_OVERLAP for 710 AstrometricParameters solutions derived from a global solution that pass Quality Control (see figure 12). The vertical dashed red line denotes the ideal level for RMS_OVERLAP of **0.05 arcsec**. Almost two-thirds of the solutions are below this accuracy limit.

4.2.2   Repeatability

As with the local solution, one method to test repeatability of the global astrometric solution is to compare the sample standard deviation of RMS values for observations of the same field using values stored in the database. This is a catalog-level comparison. A second, more robust method to test repeatability, involves comparing the sources from CoaddedRegridded-Frames derived from two separate sets of observations of the same field with maximal overlap, where the *global* astrometric solution was used to create the RegriddedFrames. The set of dithered observations used to perform this test here is taken from repeated observations of the field surrounding the Centaurus-A galaxy. Figure 14 shows residuals between the source positions extracted from two CoaddedRegriddedFrames as described in the document *Creating and analysing multi-dimensional data in Astro-WISE environment: a test case* (HTML) found on the Astro-WISE website at http://www.astro-wise.org/doc_nova.shtml. This document plots the declination residual (analogous to DDEC) versus magnitude and shows a 0.05 arcsec RMS scatter after cleaning of the most likely spurious points. Figure 14 adds the DRA component to create the familiar DDEC versus DRA plot. The two-dimensional RMS calculated from the data plotted is **0.074 arcsec**. Because the dithers were virtually on top of each other (a difference of only 50 pixels, or 10 arcsec in world coordinates), this repeatability is the **internal accuracy** of the global solution.
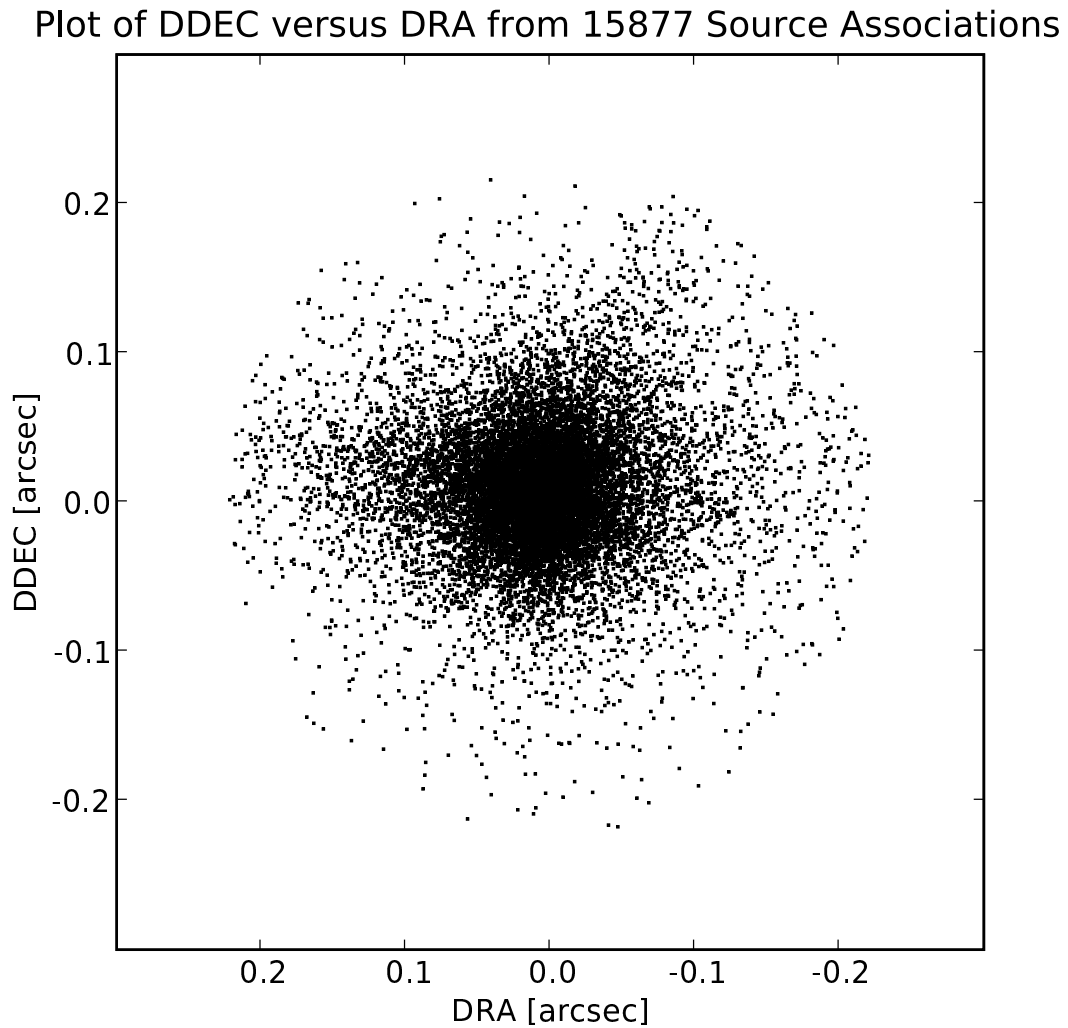
Figure 14: Example of residuals between the source positions of two CoaddedRegriddedFrames, whose source RegriddedFrames were created using the *global* astrometric solution, which have the same pointing on two nights. The data plotted has a two-dimensional RMS scatter of **0.074 arcsec** (just under a third of a pixel) for 15877 source pairings after iterative clipping at 3 times the RMS (which removes approximately 5% of the pairings). Because the two CoaddecRegriddedFrames have the same pointing, this plot illustrates the internal accuracy of the global solution. Please note, the approximately 40% increase in source associations compared to figure 8, are due to an increase in signal of each source with respect to the background, resulting from the more optimal fit.

4.3   Improvement

Now that both the local and global solutions have been thoroughly investigated individually, an overall comparison can be made of their respective performance, particularly, their solution accuracies. The method of comparing sources extracted from frames regridded using the astrometric solution throughout this report is the most robust method as it shows real-world accuracy of the solution, not only with respect to the reference or overlap sources, which can vary in both density and homogeneity across a given field, but with respect to all sources above the detection threshold (usually 10% or more than those used during the solution).

The higher the polynomial degree of the fit, the better the solution can be *for the reference sources*, but the worse it can be for those sources in the areas of the field not adequately represented by the reference sources. Comparing sources other than those participating in the solution can show whether higher polynomial degrees are adversely affecting the regions not fitted. This comparison is not relevant for this investigation and a polynomial degree of 2 for the local solutions and degree 3 for the global solutions is used in all cases.

To investigate how much the global solution improves the accuracy of the astrometric solution, the distribution of source position differences from frames regridded using the local solution are compared with the distribution of source position differences from frames regridded using the global solution. This comparison is done in two ways: using the appearance of the DDEC versus DRA plot for both the locally and globally derived residuals, and using the statistics of the two-dimensional RMS scatter between the local and global solution. The source of these statistics are the frames participating in the 27 dithers described in section 4.2.1. Each frame was used to create two RegriddedFrames, one from the local solution parameters, the other from the global solution parameters. The catalogs of all frames participating in a given global solution were then compared to each other for the local set of RegriddedFrames and for the global set separately. For each of the 27 dithers, two DDEC versus DRA plots and two RMS values were produced.

The results from the first comparison method found that for all DDEC versus DRA plots, the distributions either remained qualitatively the same (with a roughly circular distribution), or increased in their circular symmetry. Figure 15 shows an example of one of these plots (the top panel is excerpted from figure 11, but with new limits to match the lower panel). The results for the second, quantitative comparison are shown in figure 16. In this case, the 5 new dithers used a significantly different detection threshold between the local and global solutions (10 and 250, respectively), rendering any comparisons meaningless. Only the remaining 22 dithers are used here. The populations of the local RMS values and global RMS values are clearly seen. The *average* values for the two distributions are **0.10 arcsec** RMS and **0.054 arcsec** RMS, for the local and the global dataset, respectively. Please note, the values of RMS here should not be compared to the 0.04 arcsec value in the overall results. Those RMS values are based on single-chip solutions derived from the global solution. The RMS values here are based on all chips used in the global solution.

The improvement from the local to the global set is obvious and dramatic. Not only does the the scatter in source position differences decrease, any systematic offsets caused by using even slightly different areas of the reference catalog are eliminated, with a maximum improvement of a factor of more than 3 times the RMS (from 0.17 arcsec to 0.053 arcsec)! Despite this very large improvement, the **overall average improvement** for this dataset is a factor of almost **2 times**, from **0.10 arcsec** to **0.054 arcsec**. Clearly the global solution is bringing the source positions in the participating frames to near optimal alignment.
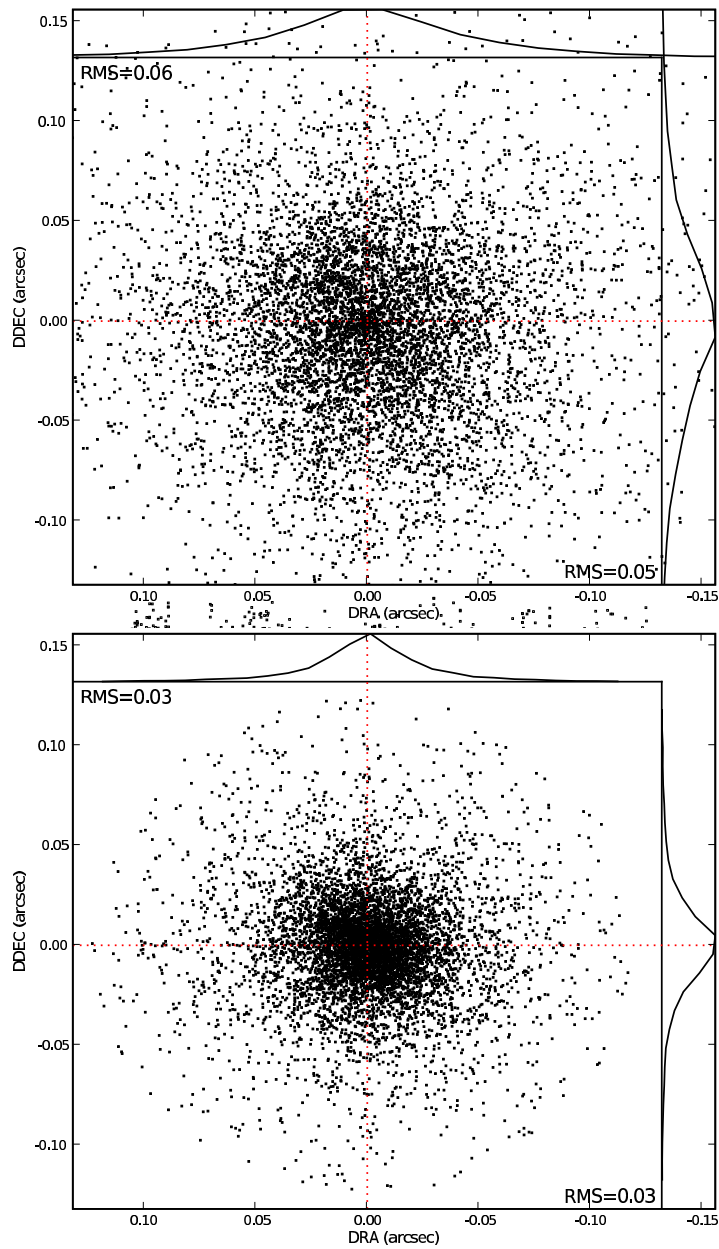
Figure 15: An example of improvement in source position alignment of the regridded frames from the local to the global solution. The source positions are those of all matching sources in any one frame and another frame, same or different chip, that overlaps the first frame. The top panel shows the overlapping source position differences from 32 frames of a 4-point dither regridded using the local astrometric solution for each frame, and the bottom panel shows the same for the same frames regridded using the global solution. The RMS value for **the** *local* **solution residuals is 0.077 arcsec** for the 7881 pairings displayed in the top panel and for **the** *global* **solution residuals is 0.041 arcsec** for the 7653 pairings in the bottom panel. This is a factor of almost two improvement. Note that some data are cropped from the upper panel due to the limits matching those of the bottom panel.

Histogram of Applied RMS for 22 Dithers
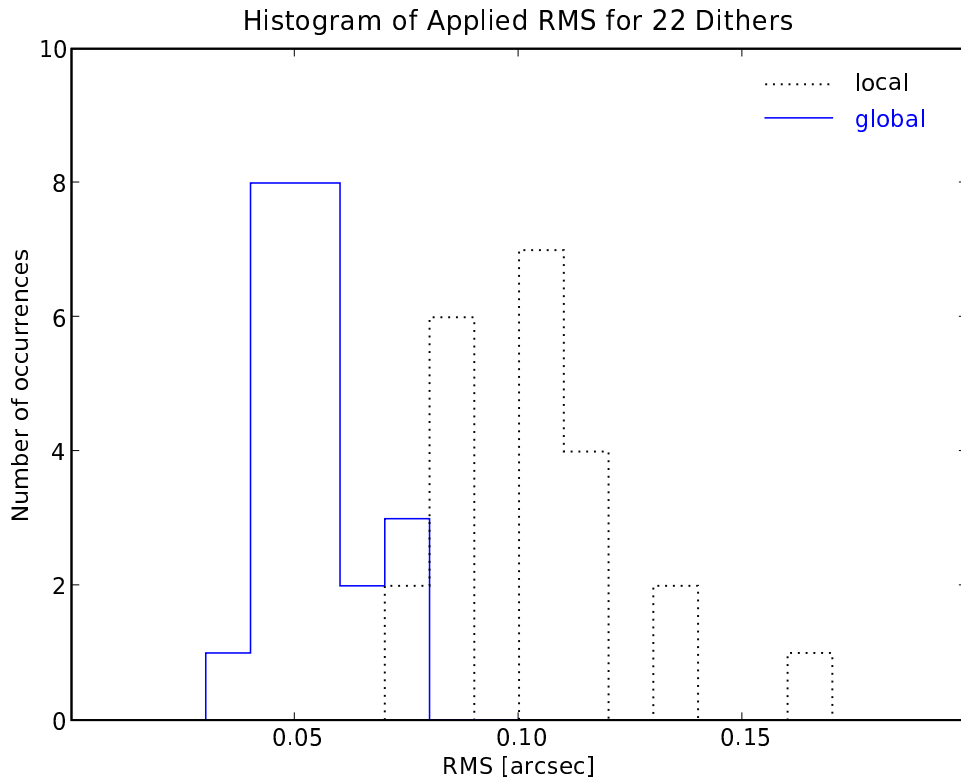
Figure 16: A histogram of the applied RMS distribution for 22 dithers. Each RMS value is calculated from the residuals of the source positions between a given chip and all overlapping chips for each dither. The source positions are extracted from frames regridded using either the local or the global solution. The histogram shows two separate distributions: the RMS values from the local solution frames (dotted black lines) and the RMS values of the global solution frames (solid blue lines). It is easy to see the difference in the distributions, with the **local** solutions' *average* RMS of **0.10 arcsec** and the **global** solutions' average RMS of **0.054 arcsec**. This shows that there is significant improvement (a factor 2 in RMS) between locally derived solutions and globally derived solutions.

4.4   Future of Global Astrometry

Currently, the global solution in Astro-WISE uses closely matched dithers and compares them to a reference catalog to obtain the most optimal balance of both relative and absolute astrometry. It may be possible in many cases to improve the astrometry of dithers that are not closely matched in either time or space, but this can only be achieved by optimizing the global astrometric process for this type of data. An investigation is currently under way to see how feasible this is (see section C).

If relative astrometry is more important than the absolute astrometry, e.g., difference imaging analysis, the standard reference catalog can be replaced with a catalog derived from one exposure of a dither. In this case, all sources in the solution will be overlap sources and any distortions with respect to the absolute reference grid will not be compensated for as they will exist in the new *reference catalog*. This relative type of global astrometry is not directly supported in Astro-WISE, but may eventually be. It is unsure if this support would take the form of a HOW-TO where the calibration scientist creates the new reference catalog, or if this functionality will be integrated into the global astrometric procedures. With the ability to solve most global solutions to an accuracy of 0.2 pixel (**0.04 arcsec**), this may be necessary only in the most demanding cases.

5   Conclusions

Astrometric calibration in Astro-WISE is robust and accurate. Local solutions typically achieve accuracies consistent with the reference catalog's accuracy of **0.3 arcsec** and global solutions typically achieve accuracies better than **0.05 arcsec**. The underlying software achieved a typical accuracy in source extraction and regridding to **one tenth of a pixel, or 0.02 arcsec**. Using the standard methods and settings, **more than 95%** of the frames processed had acceptable local solutions derived for them. The rest suffered from various data quality problems, including, but not limited to, shallow exposures, extraneous artifacts, poor initial astrometry, extended objects in the field, and very poor seeing. **All frames** processed with the global astrometric routines were successful and all achieved their target accuracy of **less than 0.1 arcsec**.

Accuracies derived from both the local and the global routines match the accuracies as applied to the pixel data. These derived accuracies are used to examine the statistics of all solutions stored in the system. These statistics show that there exists large scatter, up to 1 arcsec, for the local solution at all NREF values (number of pairings with reference sources used in the final solution). At the low NREF values, this is due to low signal-to-noise of the source pixel data and small number statistics in the least-square fit of the solution. A high NREF values, the large scatter is due to high source density and non-uniform coverage near extended sources. The population of RMS values shows a bimodal distribution that is related to frames with low exposure times. The statistics for the global solutions are far clearer to decipher with all of the solutions showing RMS values of the overlapping sources in the acceptable regime below 0.1 arcsec, more than 60% below the ideal threshold of **0.05 arcsec**.

The repeatability of the local solution was estimated to **0.085 arcsec** RMS, and the repeatability of the global solution was estimated to **0.074 arcsec** RMS. This estimation was achieved by associating catalogs extracted from frames coadded with frames regridded using the local and global solutions, respectively, of dithers overlapping to more than 99.5% taken on different nights. Inspection of source regridded frames using basic difference image analysis shows values consistent with these results.

The improvement from the local to the global solution was shown to be on average a factor of 2 in RMS from **0.10 arcsec** to **0.054 arcsec** by comparing overlapping source position differences of all frames in each dither after regridding to both the local and global solutions. The maximum improvement was more than a factor of 3 in RMS.

Lastly, the future of astrometry in Astro-WISE was explored in brief by looking at global solutions of data not currently expected to give optimal results due to poor spatial or temporal grouping (i.e., not a closely matched dither), and looking at the possibility of purely relative astrometry in the global routines.

A   Astrometry HOW-TOs

Astrometry in Astro-WISE is described in many ways in the online HOW-TOs and in the offline User and Development Manual. Below are links to the individual HOW-TOs with a brief description. If the document links do not work from your viewer, go to www.astro-wise.org, click on the *AWE Information System* tab, then on the *Howtos & Manual* tab, then the *Calibrations* and *Astrometry* links in the left menu to access the individual pages.

A.1   Drive an Astrometric Solution

This HOW-TO describes how to derive a local astrometric solution and the individual steps the LDAC programs perform to make this happen.

A.2   Create Global Astrometric SourceLists

This HOW-TO describes how to create SourceLists for the specific purpose of deriving a global astrometric solution.

A.3   Derive a Global Astrometric Solution

This HOW-TO describes how to derive a global astrometric solution.

A.4   Inspect an Astrometric Solution

This HOW-TO describes how to inspect an astrometric solution and gives detailed description and operating instructions for the inspection routines described in appendix B.

A.5   Troubleshoot an Astrometric Solution

This HOW-TO describes how to recover from a bad astrometric solution or how to improve an existing astrometric solution, whether local or global.

B   Astrometry Inspection Methods

There are a large number of ways to inspect astrometric solutions. They include looking at the residuals of corrected source positions with respect to the reference catalog source positions and to corrected overlap source positions, verifying the predicted corrections by comparing source position extracted from corrected frames (RegriddedFrames and CoaddedRegriddedFrames), and viewing spatial changes between source positions using qualitative difference and multi-color image analysis. See HOW-TO Inspect an Astrometric Solution in section A.4 for all the details.

B.1   Predicted Residuals Inspection

B.1.1   AstrometricParameters.inspect()

This plot displays the source position residuals between the corrected source positions and the USNO-A2.0 reference catalog as calculated internally by the LDAC.astrom program. This plot is for one frame only from a local or a global solution. This method was used to create figure 1.

B.1.2   GAstrometric.inspect()

This plot displays the source position residuals between the corrected source positions and between the USNO-A2.0 reference catalog as calculated internally by the LDAC.astrom program. This plot is for all frames participating in a global solution only. This method was used to create figure 10.

B.2   Applied Residuals Inspection

B.2.1   AstrometricParameters.plot_residuals_to_usno()

This plot displays source position residuals between the corrected catalog positions performed by LDAC or sources positions extracted from a RegriddedFrame corrected with the same parameters, and the USNO-A2.0 reference catalog. This method was used to create figure 3 (with option source='applied').

B.2.2   AstrometricParameters.plot_residuals_to_regrid()

This plot displays source position residuals between the corrected catalog positions performed by either LDAC or SExtractor and sources extracted from a RegriddedFrame corrected with the same parameters. This method was used to create figure 2 (with option derived_type='solution').

B.2.3   CoaddedRegriddedFrame.plot_regrid_residuals()

This plot displays source position residuals between a given RegriddedFrame and all other overlapping frames, all that participate in a CoaddedRegriddedFrame. Setting the use_coadd switch (use_coadd=True) displays source position residuals between the CoaddedRegriddedFrame and all RegriddedFrames that went into its creation. It plots a given RegriddedFrame source position against the average source position from the CoaddedRegriddedFrame. This method was

used to create figures 11 & 15 (with option use_coadd=False), and figures 17, 18, 19, & 20 (with option use_coadd=True).

B.3   Image Inspection

B.3.1   BaseFrame.inspect(compare=True)

This plot can be used to display the qualitative residuals on the pixel level by using either difference images or multi-color images using the same mechanism for inspecting individual frames. This method was used to create figure 9 (with option compare=True and option color=False).

C   Global Astrometry in the DEEP3a Field: A Case Study

Global astrometry in ASTRO-WISE is taking advantage of fixed focal-plane geometry applicable under certain conditions for WFI, and likely more commonly applicable for OmegaCAM. This means that any difference in the focal-plane geometry from pointing to pointing is assumed to change in a linear fashion only, with higher order distortions remaining constant (e.g., only relative translations of the entire focal plane in RA and Dec are corrected for). When valid, this assumption of fixed focal-plane geometry adds information to the system, benefitting the astrometric solution. Generally, only closely matched sets of exposures taken within strict temporal limits[11] (for WFI, approximately less than one hour between first and last exposure) will demonstrate a fixed focal-plane geometry. This condition minimizes differences in telescope flexure caused by different altitude and azimuth locations.

C.1   The Data

A subset of the WFI DEEP3a data currently existing in the ASTRO-WISE system is used in this study. This subset has the following characteristics: 30 exposures taken over 9 days in the R-band, centered at sky coordinates $\alpha = 11h24m48s$ and $\delta = -21d41m39s$ with less than 70% total overlap, all with seeing below 2 arcsec, and airmass between 1.012 and 1.325 (zenith distance, or ZD, of between 8.8 and 41 degrees). The exposures can be sub-divided into two distinct groups of 19 low ZD exposures (8.8 to 18.9 degrees, or airmass of 1.012 to 1.057) and 11 high ZD exposures (24 to 41 degrees, or airmass of 1.096 to 1.325). This distinction is important because the highest quality solutions are obtainable for only closely matched sets of exposures. These high differences in ZD imply large differences in flexure for this telescope, and therefore, large differences in higher order distortions. Overlap of all frames of less than 70% complicates matters further by reducing the number of sources common to all exposures.

C.2   The Solutions

The standard method in ASTRO-WISE of combining multiple sets of closely matched exposures is to obtain global solution for each set independently. The independently derived solutions can be applied to the source frames to create frames regridded to the same grid target (spatial reference point on a fixed grid). These regridded frames can then be coadded together to create the final combination (e.g., using SWarp, Eclipse, or PyFITS/NumPy for the image combination).

Individual global solutions for three N=5 dithers and one N=3 dither from the low ZD dataset were obtained using a plate polynomial of degree 3. These solutions were applied to obtain 144 regrids. The regrids were stacked (coadded) by dither to create four frames and **the mean RMS of the individual regrids with respect to the four coadds is 0.034 arcsec** (see figure 17 for an example). The mean full width at half maximum (FWHM) obtained from the Gaussian profile fits of the DRA and DDEC distributions gives the values of **0.039 arcsec and 0.032 arcsec**, respectively.

The 144 regrids were then coadded into one frame and **the RMS of the individual regrids with respect to the single coadd is 0.060 arcsec** (see figure 18). The FWHM of the fit to these DRA and DDEC distributions gives the values of **0.067 arcsec and 0.077 arcsec**, respectively.

---

[11]Strict spatial limits also aid in the global solution, but are not a condition for a fixed focal-plane geometry. The most optimal results are derived from sets of exposures with greater than 90% overlap due to the larger number of sources common to all exposures.

Lastly, a single global solution for the three N=5 dithers and the one N=3 dither was obtained using a plate polynomial of degree 3, with the assumption that the entire set meets the fixed focal-plane geometry argument. This solution was applied to obtain 144 regrids that were coadded to obtain the **RMS value of 0.056 arcsec** (see figure 19). The fitted FWHM values for DRA and DDEC are now **0.076 and 0.069 arcsec**, respectively.

C.3 Tuning for Optimal Results

The DEEP3a dataset in question here is obviously not optimal for the default settings of the Astro-WISE environment given the increase in RMS from the single dither solutions to the multi-dither solutions (see section C.2). It requires significant manual *tweaking* to get a the optimal solution. This is due mostly to the large temporal separation (9 days) and large spatial separation (less than 70% overlap of all frames) of the dataset. The distortion and overlap information is not adding information in a beneficial way, and requires the configuration parameters to be modified far from their default settings.

One global solution was obtained for the three N=5 dithers and the one N=3 dither using a plate polynomial of degree 3 and increasing the order of the Chebychev (pointing-to-pointing) polynomials[12] from their default of [1,0,0] to [1,15,15]. This solution was applied to obtain 144 regrids that were coadded to obtain the **RMS value of 0.034** (see figure 20). The fitted FWHM values for DRA and DDEC have improved to **0.039 and 0.032 arcsec**, respectively.

---

[12]The Chebychev polynomials control the degrees of freedom of the pointing-to-pointing solution parameters such that a value of [1,0,0] allows the linear terms of the plate polynomial to vary linearly, while fixing the higher order terms of the plate polynomial. Setting the last two values to non-zero values unfixes the higher order terms, allowing compensation for combinations not meeting the fixed focal-plane geometry assumption.

Figure 17: Residuals of the source positions extracted from the regridded frames with respect to the source positions extracted from the coadded frame created from the same regridded frames. The residuals here are from frames regridded using one global solution for all CCDs of 5 exposures taken over approximately an hour. The RMS for this plot is **0.034 arcsec** for 10987 source parings.

Figure 18: Residuals of the source positions extracted from the regridded frames with respect to the source positions extracted from the coadded frame created from the same regridded frames. The residuals here are from frames regridded using 4 different global solutions for all CCDs of 18 exposures taken over a week and a half. The RMS for this plot is **0.060 arcsec** for 42902 source parings.

Figure 19: Residuals of the source positions extracted from the regridded frames with respect to the source positions extracted from the coadded frame created from the same regridded frames. The residuals here are from frames regridded using one global solution for all CCDs of 18 exposures taken over a week and a half. The RMS for this plot is **0.056 arcsec** for 42769 source parings.
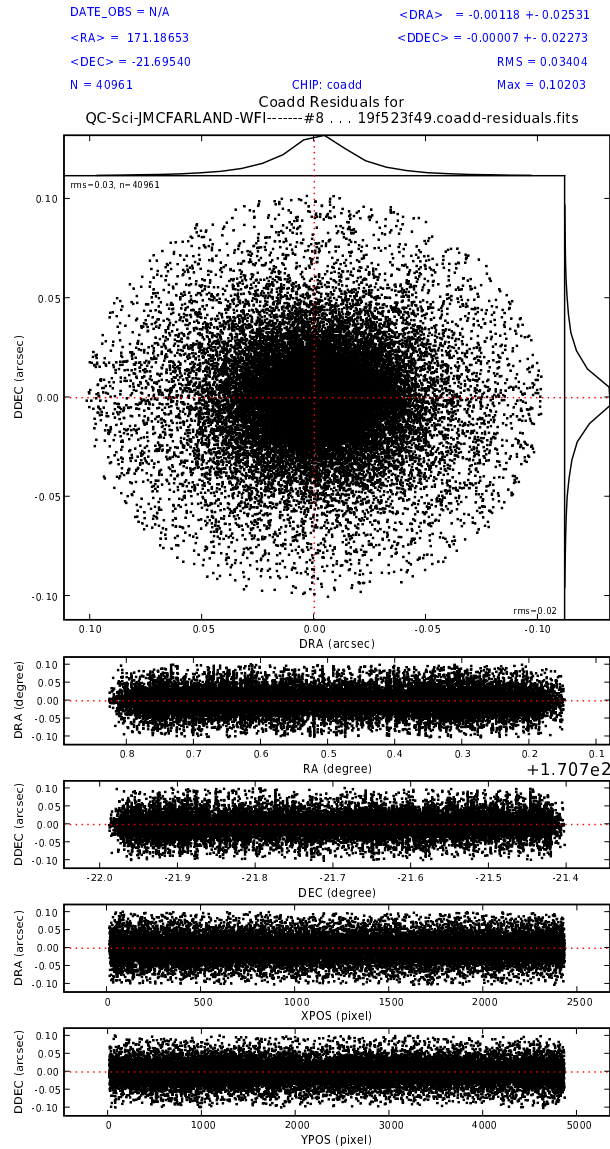
Figure 20: Residuals of the source positions extracted from the regridded frames with respect to the source positions extracted from the coadded frame created from the same regridded frames. The residuals here are from frames regridded using one global solution for all CCDs of 18 exposures taken over a week and a half, where the pointing-to-pointing differences in distortions are accounted for. The RMS for this plot is **0.034 arcsec** for 40961 source parings.

C.4   Discussion

The standard method of combining exposures in Astro-WISE utilizes the extra information in a given set of exposures. This works best when the assumption of fixed focal-plane geometry is valid. For the individual, low ZD dithers of the DEEP3a data, this assumption is indeed valid. However, for the combination of the individual dithers, this assumption appears not to be valid. The RMS of these results is nearly double the mean RMS of the individual dithers. Whether this combination is accomplished using one or multiple global solutions, the results are similar (see section C.2).

This combination method *can* extend to the set of higher ZD observations, although with yet poorer results. The scatter in the residuals is expectedly worse given the larger scatter in ZD which causes a larger difference in the higher order distortions between exposures. This scenario is not recommended and is definitely not supported under the fixed focal-plane geometry assumption upon which Astro-WISE global astrometry is built. Obviously, combining both low *and* high ZD observations would also violate this assumption.

Given these arguments, it is still possible to handle this type of data combination in Astro-WISE. The only way to achieve this is to increase the order of the Chebychev (pointing-to-pointing) polynomials (via the process parameter FDEG) which allows the higher order terms to vary in the solution, thus compensating for the differences in higher order distortions (see section A.5 for more information on how to change the appropriate settings). This method was seen in section C.3 to improve the RMS of the combination to the level of the individual dithers[13]. *It must be stressed that only non-standard combinations not fulfilling the fixed focal-plane geometry assumption require this type of treatment to achieve the most optimal results.*

Please note, using the diagnostic of plotting the differences between the source positions extracted from the regrids and the source position extracted from the coadd was used to measure the consistency of the regrids and to compare to a previous study of this data. This is not the normal or recommended method to measure this consistency. Comparing the source positions of any regrid to the same source positions on all of the other regrids is the default method used in Astro-WISE for this type of comparison. The regrids-to-coadd method underestimates the scatter by up to a factor of two because the comparisons are to the average positions of all regrids as extracted from the coadd.

C.5   Conclusions

The combination of a subset of the DEEP3a data is accomplished in Astro-WISE using multiple methods, both standard and non-standard. The standard methods work well provided the fixed focal-plane assumption is valid. This is the case for only the individual dithers, where a **mean RMS value of 0.034 arcsec** was obtained. For the combination using multiple global solutions, the **RMS value obtained increased to 0.060 arcsec**, and for the combination using only one global solution, the **RMS value of 0.056 arcsec** was obtained. This result was expected, showing that the two combination methods are equivalent. Obviously, the results of the combinations are not as good as the completely individual results, so optimization of the combination was obtained. The result for this optimized combination had the **RMS value of 0.034 arcsec**, on the same level as the RMS values of the individual dithers.

---

[13]Only the results for the 18 exposures with FDEG=[1,15,15] is shown here for consistency. The result for all 30 exposures was comparable, with a RMS value of 0.061 arcsec and FWHM values for DRA and DDEC of 0.071 and 0.054 arcsec, respectively. With the larger spread in ZD, there is obviously room for improvement.